Hindawi Publishing Corporation
Journal of Nanomaterials
Volume 2012, Article ID 895131, 8 pages
doi:10.1155/2012/895131

Research Article

Elastic Modulus Determination of Al-Cu Film Alloys Prepared by Thermal Diffusion

E. Huerta,[1,2] A. I. Oliva,[1] F. Avilés,[3] J. González-Hernández,[2] and J. E. Corona[1]

[1] *Departamento de Física Aplicada, Centro de Investigación y de Estudios Avanzados del IPN Unidad-Mérida, A.P. 73-Cordemex, 97310 Mérida, YUC, Mexico*
[2] *Materiales Nanoestructurados, Centro de Investigación en Materiales Avanzados, S.C., Avenida Miguel de Cervantes 120, Complejo Industrial Chihuahua, 31109 Chihuahua, CHIH, Mexico*
[3] *Unidad de Materiales, Centro de Investigación Científica de Yucatán A.C., Calle 43 No. 130 Col. Chuburná de Hidalgo, 97200 Mérida, YUC, Mexico*

Correspondence should be addressed to E. Huerta, microsco@mda.cinvestav.mx

Received 8 May 2012; Accepted 19 June 2012

Academic Editor: Hamed Bahmanpour

Elastic moduli of 50–250 nm thick Al-50 at % Cu film alloys deposited by thermal evaporation on Kapton substrates and postformed by thermal diffusion are investigated. Formation of the Al_2Cu alloy phase was confirmed by X-ray photoelectron spectroscopy (XPS). Surface morphology was examined by atomic force microscopy (AFM) and scanning electron microscopy (SEM) before and after tensile mechanical testing. Force-strain curves of the Al-Cu alloy were obtained by subtracting the effect of the force-strain Kapton curves from the corresponding curves of the Al-Cu/Kapton system. A reduction in the elastic modulus of the Al-Cu alloys from 106.1 to 77.8 GPa with the increase of alloy thickness was obtained. Measured elastic moduli were between the reported bulk modulus for Al and Cu. Reductions in the surface roughness and increments in the grain size were measured after tensile testing of the Al-Cu alloys.

1. Introduction

The current tendency in the electronic industry is to use flexible polymers as substrates to fabricate electronic circuits, rendering portable, low-cost, low-weight, and flexible electronic devices. For this reason, it is necessary to determine and understand the behavior of the physical properties of nanofilms deposited on flexible substrates [1, 2]. Particular attention needs to be paid to the understanding of the mechanical properties, especially the elastic modulus. Among the different methods used to estimate the elastic modulus of thin film materials are those based on vibrations [3], tensile [4], and bending testing [5]. In the electronic industry, the aluminum-copper alloys (Al-Cu) are used as metallic interconnectors [6], because of the reduction of the electromigration effects in aluminum [7]. The inclusion of polymeric materials as substrates in the electronic devices fabrication makes the interconnectors and electronic components suffer strains by Joule effect during their operation. Thus, it is important to study the mechanical behavior of these devices by knowing the elastic modulus of the interconnector materials at nanothicknesses for improving their performance. Figure 1 shows the Al-Cu alloy phase diagram in bulk [8, 9] where different phases can be observed. Al-Cu alloy phases β_0, β, γ_0, and ε_2 are formed from 1373 to 823 K, while θ (Al_2Cu) [10], η_1 (AlCu), ξ_2 (Al_3Cu_4), δ (Al_2Cu_3), and γ_1 (Al_4Cu_9) appear as stable phases below 823 K. As can be seen, the formation of the different phases is mainly determinated by the concentration of each element and the cooling rate during solidification [11, 12]. An important crystallographic phase with adequate electrical characteristics for the microelectronic industry is the AlCu phase (η_1), which is a stoichiometric phase formed below 823 K.

In this work, the elastic modulus of Al-50 at. % Cu alloy films with 50–250 nm thickness, prepared by thermal evaporation on Kapton 50HN flexible substrates and post thermal diffusion, is investigated. The morphology and

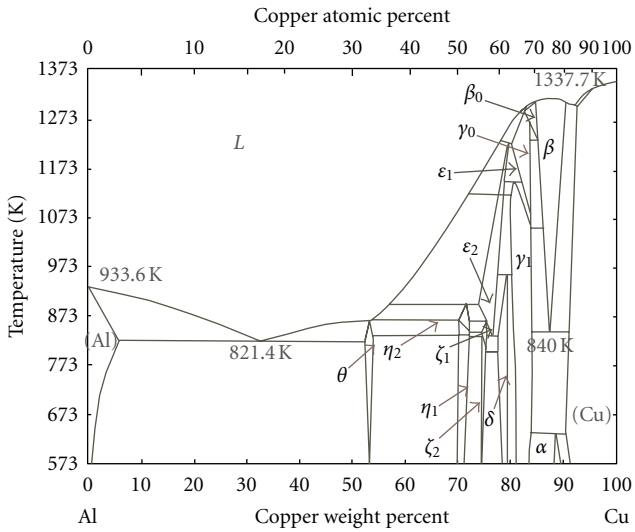

Figure 1: Phase diagram of the bulk Al-Cu alloy.

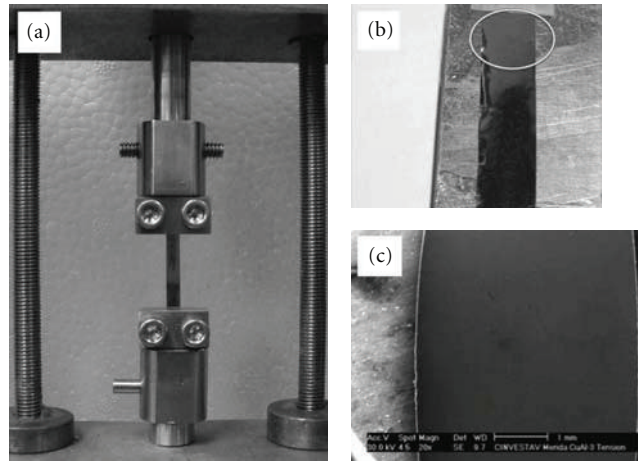

Figure 2: (a) Sample pressed by the clamps, (b) detail of the sample surface after tensile testing, and (c) micrograph of the nondamaged grip zone of the sample.

mechanical properties of the Kapton foil substrate and metallic alloys were investigated in order to determine features and properties of the formed Al-Cu alloy from differences with the bare substrate. Pure Al and Cu 50 nm thickfilms were also analyzed for comparison.

2. Materials and Methods

2.1. Alloys Preparation and Substrate Selection. For Al-Cu alloys preparation, high-purity Cu (99.999%) from CERAC was first deposited on 12.5 μm thick Kapton (50HN) foil substrates by thermal evaporation into a vacuum chamber with a pressure of 6.0×10^{-5} Torr and a deposition rate of 0.2 nm/s. Film thickness and deposition rate were measured and monitored in situ with a TM-400 controller with a quartz crystal sensor. High-purity Al (99.999%) was subsequently deposited on the Cu/Kapton system, forming an Al/Cu bilayer on top of the Kapton substrate. The chosen order of deposition is related to the rapid and continuous oxidation of Cu in comparison with the high stability of the Al oxide. The Al-Cu alloys were prepared with a nominal 50 : 50% atomic concentration and deposited with 50, 100, 150, 200, and 250 nm as total thickness. The corresponding individual film thicknesses for this atomic concentration were calculated as t_{Al} = 58.4% and t_{Cu} = 41.6% of the total thickness. Four samples were simultaneously deposited for each batch. Once the bilayers were formed, Al-Cu alloys were post-formed by thermal diffusion at 673 K by a thermal annealing process during 3 h into a vacuum oven with Argon gas to avoid oxidation. The natural cooling process of the oven, from 673 K to 313 K, required 2 additional hours of the films into the Argon atmosphere. Due to the annealing process, the Al-Cu/Kapton alloys suffered thermal stresses as observed by curling of the samples. The residual stress is assumed to arise from shrinkage of the substrate up to 1% at 673 K (as reported by the supplier) and by the thermal diffusion of the material [13–16]. Additionally, 50 nm thick samples of only Al and only Cu were thermally deposited to prepare Al/Kapton and Cu/Kapton systems to be used as references. Kapton was selected as the substrate material due to its high melting temperature, smooth surface, and relatively low elastic modulus. The surfaces morphology of Kapton as-received and after thermal annealing at 673 K as well as used for the metallic alloys were examined by atomic force microscopy (AFM) in tapping-mode. AFM images of $2 \times 2\,\mu m^2$ size, 512×512 pixels^2 of resolution, and 1 Hz as scanning rate were obtained. Preliminary results of the mechanical properties of Kapton 50HN substrates and Al-Cu/Kapton alloys were reported [17] and determined from strain-stress curves obtained from a homemade universal testing machine [18] with a load cell of 220 N. The sample strain was measured by using the machine cross-head displacement, taking into account the compliance of the universal testing machine. The machine compliance, estimated as 0.16 μm/N, is small enough to avoid affectation on the elastic modulus determination. Tensile tests of samples were performed with a cross-head speed of 1 μm/s (strain rate of 6.0×10^{-5} s^{-1}). The gauge length (distance between clamps) used for the tensile testing machine was 20 mm. Samples of rectangular geometry of 40 mm length and 4 mm wide were used for tensile tests. No damages with the clamps were produced on the sample surfaces after tensile testing during sample holding. This can be observed in Figure 2, where a sample pressed by the clamps is shown (Figure 2(a)); meanwhile in Figures 2(b) and 2(c), micrographs of the nondamaged grip zone of the sample after the tensile testing can be observed with different magnifications.

2.2. Characterization of the Al-Cu Alloys. Phases of the Al-Cu alloy were investigated by X-ray photoelectron spectroscopy (XPS). XPS analysis was performed by an ESCA/SAM 560 Perkin-Elmer equipment. The analysis was performed at 0.5–3.0 nm-depth from the sample surface (about 3 atomic layers), given the erosion rate used during analysis. Images of the surface morphology of the Al-Cu alloys surfaces

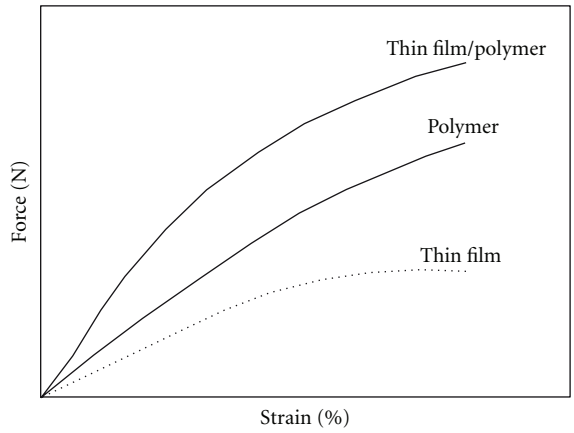

Figure 3: Force-strain curves of the thin film/polymer and polymer substrate systems, and the corresponding thin film curve obtained by subtraction.

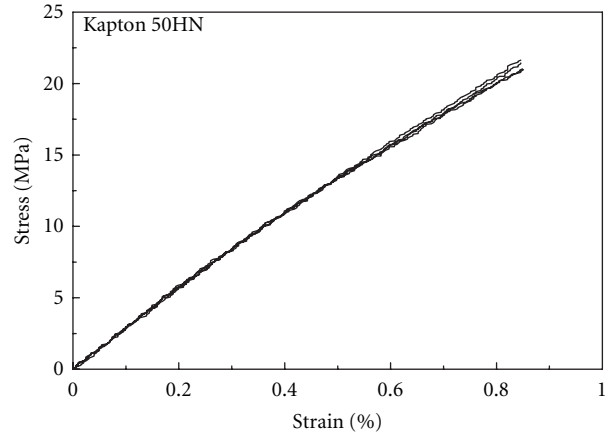

Figure 5: Four stress-strain curves obtained for 12.5 μm thick Kapton substrate after thermal annealing and etching. A high reproducibility was observed from the tensile tests presented in the plot.

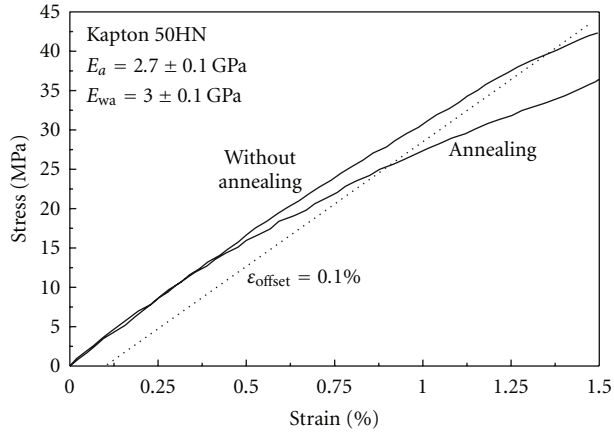

Figure 4: Stress-strain curves of 12.5 μm thick Kapton foil for as-received and after thermal annealing.

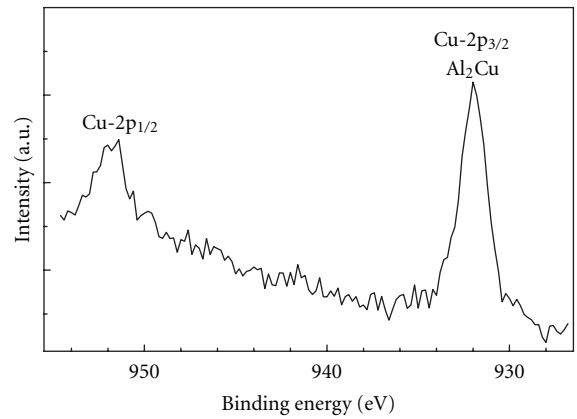

Figure 6: XPS spectrum as obtained for an Al-50 at % Cu alloy sample.

were examined by atomic force microscopy (AFM). Rms-roughness (R_{rms}) and grain size (D) before and after the tensile tests were measured using the scanning probe image processor (SPIP) software from Image Metrology Co. The microstructure of the Al-Cu alloys was examined by a scanning electron microscopy (SEM), both by secondary electrons (surface) and by backscattered electrons (to identify elemental composition on different zones of the alloy) with 25 keV using a SEM-Philips XL30 ESEM. Additionally, elemental concentration from different zones of the formed alloys was measured by energy dispersive spectroscopy (EDS).

2.3. Elastic Modulus of the Al-Cu Alloys. Two tensile tests were carried out for each system, one with the metallic alloy/substrate and the second one without the metallic film. The first tensile test was carried out to the Al-Cu alloy bonded to the Kapton substrate to obtain the force-strain curve of the complete Al-Cu/Kapton system. The Al-Cu film alloy was then removed from the Kapton substrate by etching the alloy during 5 minutes into a weak sulfuric acid solution. This process etched the metallic film without affecting the elastic modulus of the substrate as was confirmed by the tensile testings of the Kapton substrates before and after film etching. The second tensile test was subsequently performed to the etched substrate to obtain the force-strain curve of the bare substrate. The tensile stress (σ) of the alloy as a function of applied strain (ε) was calculated by subtracting the force-strain curve of the Kapton substrate $F_{sub}(\varepsilon)$, from the force-strain curve corresponding to the Al-Cu/Kapton foil $F_{tot}(\varepsilon)$, according to the relation [19],

$$\sigma(\varepsilon) = \frac{1}{t_f w_f}[F_{tot}(\varepsilon) - F_{sub}(\varepsilon)], \quad (1)$$

where t_f and w_f are the thickness and width of the alloy, respectively. Force-strain curves of the thin film/polymer system, polymer substrate, and the thin film curve, used to obtain the mechanical properties of the thin films, are plotted in Figure 3. The lower dashed-line curve in Figure 3 corresponds to the curve of the thin film, which was

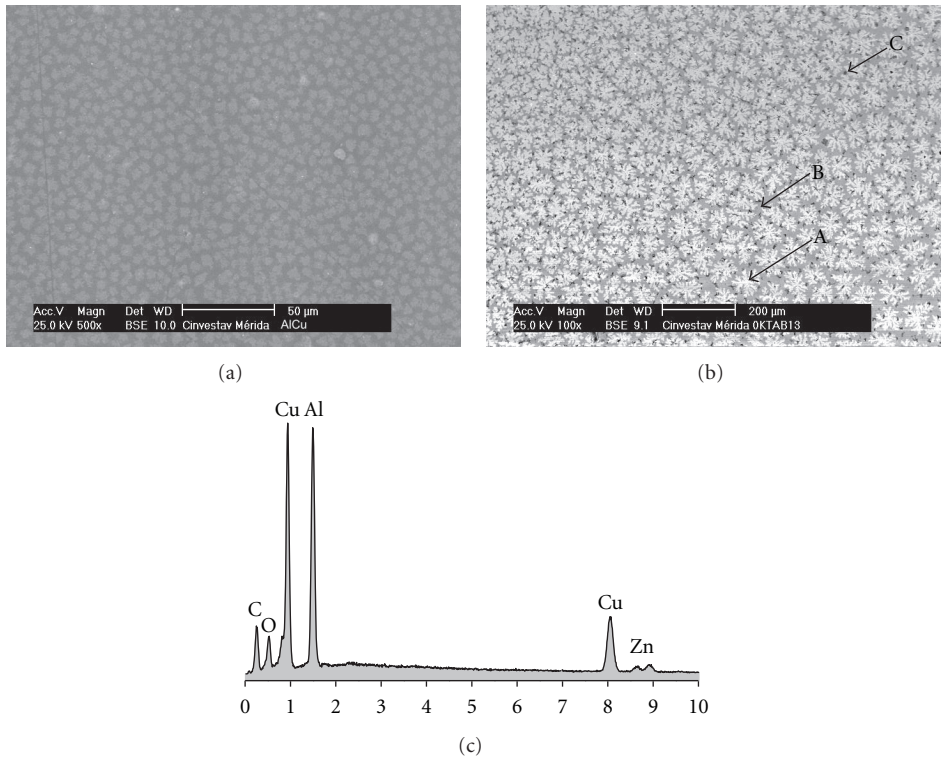

Figure 7: SEM images showing the microstructure evolution when the sample is annealed: (a) 1 h to (b) 3 h. (c) EDS results corresponding to the sample annealed for 3 h.

obtained by subtracting the measured force-strain curve of the polymer substrate from the force-strain curve of the thin film/polymer system.

Additionally, batches of only Al and Cu films of 50 nm thick deposited on similar Kapton substrates were analyzed by this method to estimate thier corresponding elastic modulus.

3. Results and Discussion

3.1. Substrate Analysis. The surface morphology of Kapton substrate both before and after the annealing process was measured by AFM, finding no significant changes in the rms-roughness. Rms-roughness values of the Kapton surface were determined in a range of 1.1–2.9 nm, confirming that Kapton foil presents a uniform low-roughness surface which is suitable to use as a substrate for depositing alloy films with uniform thickness and low-roughness. Additionally, the mechanical properties of Kapton substrates were examined before and after thermal annealing. Figure 4 shows two stress-strain curves from Kapton foil obtained from as-received, and after 3 h of annealing treatment. Both as-received and annealed Kapton foil present an initial linear elastic behavior for low strain values ($\varepsilon \leq 1.3\%$). The rule of $\varepsilon = 0.1\%$ offset applied to both stress-strain curves yields deviations from linearity at $\varepsilon = 1.3\%$ for the as-received Kapton and $\varepsilon = 0.9\%$ for the annealed Kapton.

The corresponding elastic moduli were estimated by fitting a straight line into this region. The corresponding mean value of the elastic modulus obtained in this way for as-received Kapton is $E_{wa} = 3.0 \pm 0.1$ GPa, meanwhile for annealed Kapton is $E_a = 2.7 \pm 0.1$ GPa, that is, a reduction of elastic modulus of ~10% for the annealed Kapton. This slight reduction of the elastic modulus was taken into account to estimate the elastic modulus of the Al-Cu alloys, such that the annealed curve was used for subsequent calculations. For the case of pure metallic films (Cu and Al), the elastic modulus was estimated using the mechanical properties of as-received Kapton since no annealing process is involved. Figure 5 shows the stress-strain curves corresponding to the elastic zone of only Kapton obtained after 3 h of thermal annealing and etching during 5 minutes into a weak sulfuric acid solution. The obtained stress-strain curves of the substrate show high reproducibility for the different replicates tested. For all tensile tests, a strain range of 0.9% was used to estimate the elastic modulus. Negligible variations in the estimated elastic modulus of the annealed Kapton (E_a= 2.7 GPa) after etching into a weak sulfuric acid solution were observed. At this strain range, Kapton substrate is into the elastic zone and does not suffer damage that can affect the mechanical properties of the films. Once Kapton substrate was characterized, the tensile tests of the Al-Cu/Kapton system were conducted.

3.2. Phase Alloy Analysis. The formed phases of the prepared Al-Cu/Kapton alloys were determined by XPS. XPS spectra in the 1000–0 eV energy range were obtained. Subsequent high-resolution XPS spectra of Al-2p, Cu-2$p_{1/2}$, and Cu-2$p_{3/2}$

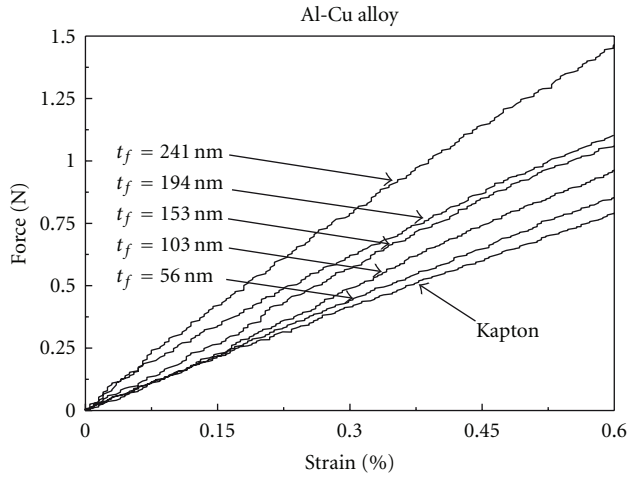

Figure 8: Measured force-strain curves of Kapton foil and Al-Cu/Kapton systems for different thicknesses. Thickness values correspond to the deposited values.

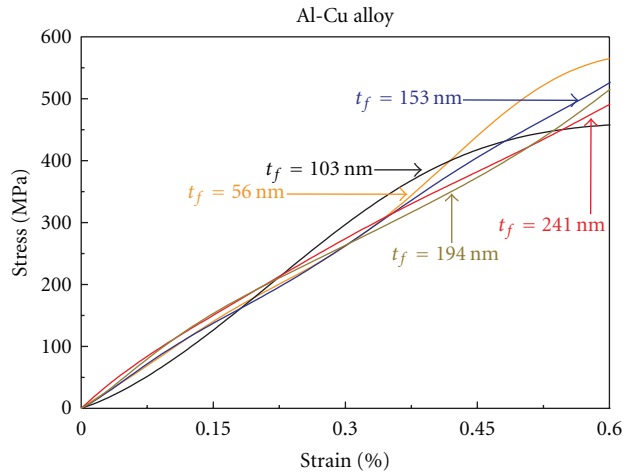

Figure 9: (color online) Stress-strain curves as obtained for Al-50 at % Cu alloys with different thicknesses.

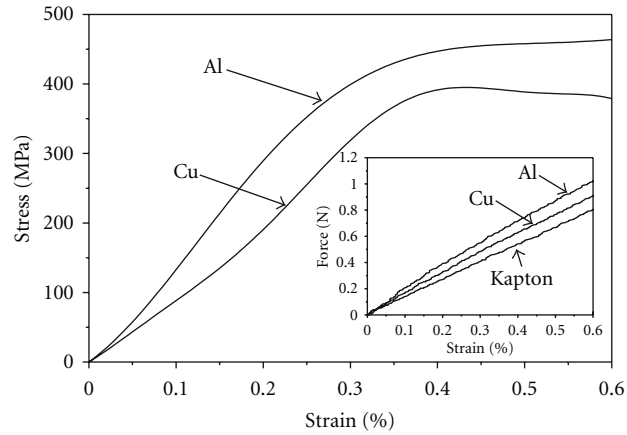

Figure 10: Stress-strain curves for 50 nm-thick of Al and Cu. Inset shows the corresponding force-strain curve.

were determined, as is shown in Figure 6. The main Al peak (Al-2p) appearing at 74 eV (not shown) corresponds to an oxidized state of Al. The Cu spectrum consists of a set of $2p_{1/2}$ and $2p_{3/2}$ peaks, associated to the Al_2Cu phase [20]. According to the Al-Cu bulk phases diagram for an Al-50 *at* % Cu, the expected phase is AlCu. However, Al_2Cu phase may also be produced during the cooling process [21].

3.3. Microstructure and Morphology of Al-Cu Alloys. The microstructure of the Al-Cu alloys was analyzed by EDS-SEM technique using the backscattered secondary electrons mode. Figures 7(a) and 7(b) show two SEM images of the alloy microstructure after the annealing time of 1 h and 3 h, respectively. As can be observed in Figure 7(a) the alloy is not formed completely given the minor time of the annealed treatment. Microstructure of the alloy annealed during 3 h shows to be more homogeneous than for annealed films after 1 h. Figure 7(b) shows three analyzed zones of the Al-Cu alloy which was labeled as: white zone (A), gray zone (B), and dark points (C). Zone A is characterized by the dendritic structures. Stoichiometry of the zone A yields concentrations of Al = 41.7% at and Cu = 58.3% at. Zone B is characterized by the peripherical dendritic structures, with atomic concentration of Al = 46.0% and Cu = 54.0%. Dark points C, with concentrations of Al = 53.2% and Cu = 46.8%, are characterized by the highest concentration of aluminum. From EDS analysis, zone A was found to be richer of Cu than the B and C zones. Figure 7(c) shows an EDS general analysis of the sample annealed for 3 h. Additionally, evidence of diffusion of Cu or Al into the Kapton foil during the annealing process was not found, which was confirmed by the EDS analysis carried out in localized areas of the Kapton where the Al-Cu alloy was removed.

3.4. Alloys Tensile Tests. Figure 8 shows representative force-strain curves of the Al-Cu/Kapton system deposited with different film thicknesses (t_f = 50 to 250 nm, nominal values) and of neat Kapton substrate as the baseline. Representative force-strain curves from four samples for each Al-Cu/Kapton system and the corresponding curve for Kapton substrate are included.

Reported thickness values correspond to the deposited thicknesses of the formed Al-Cu alloy as measured by the quartz crystal sensor during thermal evaporation. As can be observed, the slope of the force-strain curve increases as the film thickness increases. The corresponding stress-strain curves of the Al-Cu alloys prepared with different thickness were calculated using Figure 8 and Equation (1) and are shown in Figure 9. From each curve of Figure 9, the elastic moduli of different Al-Cu alloys were estimated.

The elastic modulus values were estimated as the initial slope of the straight line of each curve in the range of $0 \leq \varepsilon \leq 0.6\%$, that is, within the linear elastic regime. The mean values and the corresponding standard deviations estimated

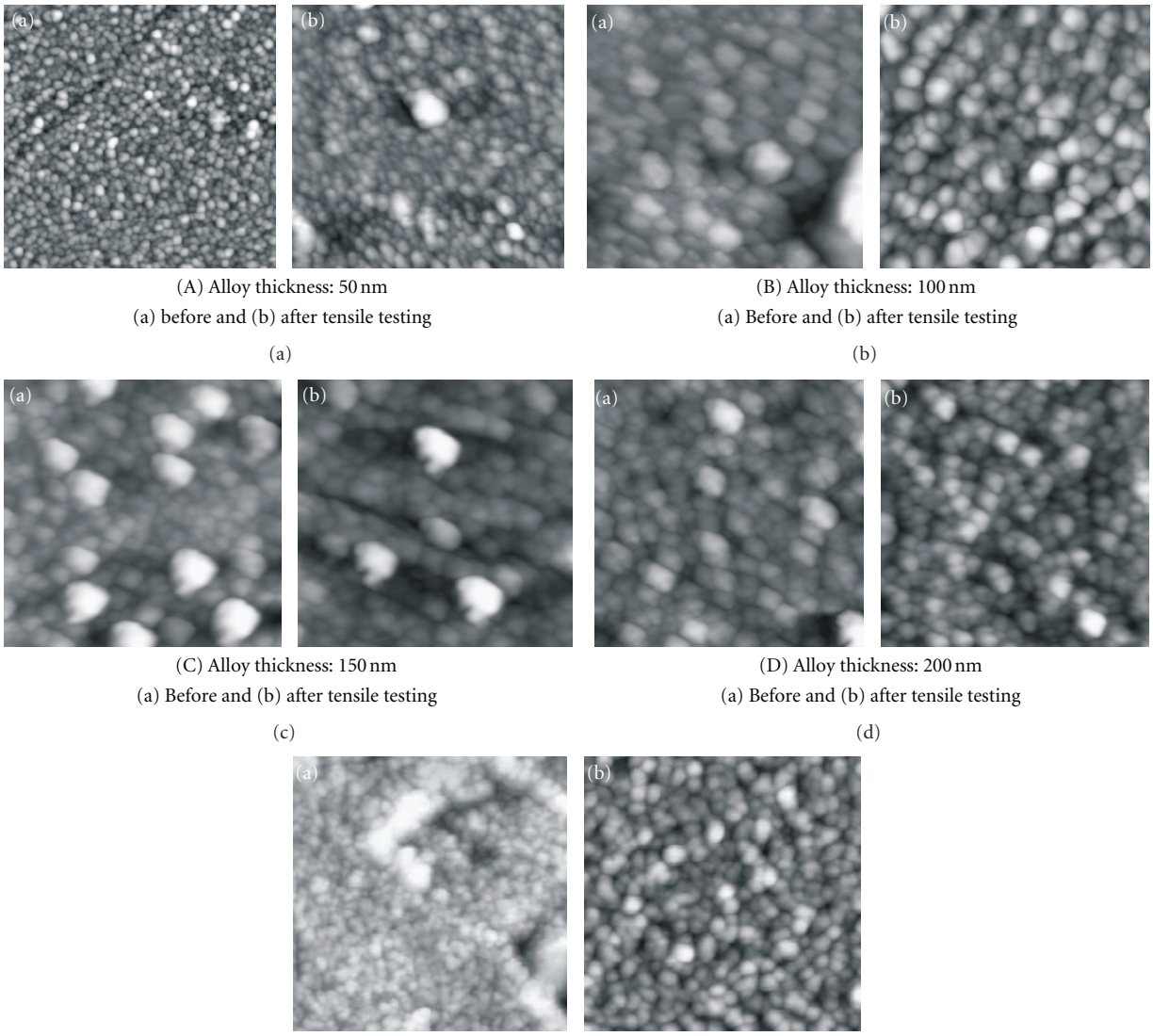

Figure 11: AFM images ($2 \times 2\,\mu m^2$) of the Al-Cu film morphology for different thicknesses, before and after tensile testing, (A) 50 nm, (B) 100 nm, (C) 150 nm, (D) 200 nm, and (E) 250 nm.

Table 1: The mean elastic modulus of Al-Cu alloys, Al and Cu with different thickness.

Thickness (nm)	Al-Cu (GPa)	Al (GPa)	Cu (GPa)
50	104.6 ± 6.2	129.1 ± 4.2	107.1 ± 4.6
100	99.1 ± 1.8	—	—
150	106.1 ± 5.5	—	—
200	77.8 ± 1.6	—	—
250	82.7 ± 5.6	—	—

for the elastic modulus are shown in Table 1. From Table 1, it can be observed that the elastic modulus decreases as the alloy thickness increases. Table 1 also includes the elastic modulus as obtained for 50 nm thickness of Al and Cu films.

As known, the reported elastic modulus for Al and Cu in bulk is 70 and 130 GPa, respectively [22]. The elastic moduli of the Al-Cu film alloys fall between the bulk moduli of Al and Cu, approaching to the bulk modulus of Al as the alloy thickness increases. Additionally, the elastic moduli of 50 nm thick thermally evaporated samples of Al/Kapton and Cu/Kapton were measured for comparison. The corresponding stress-strain curves of 50 nm thick Al and Cu are shown in Figure 10. These curves were obtained from the force-strain curves shown inset. For Al films, a mean elastic modulus of 129.1 ± 4.2 GPa was obtained, a significantly higher value than its bulk value (70 GPa).

The obtained elastic modulus for Cu films was 107.1 ± 4.6 GPa, a lower value as compared with its bulk value (130 GPa). Values of 108.8 ± 11.7 GPa of the elastic modulus

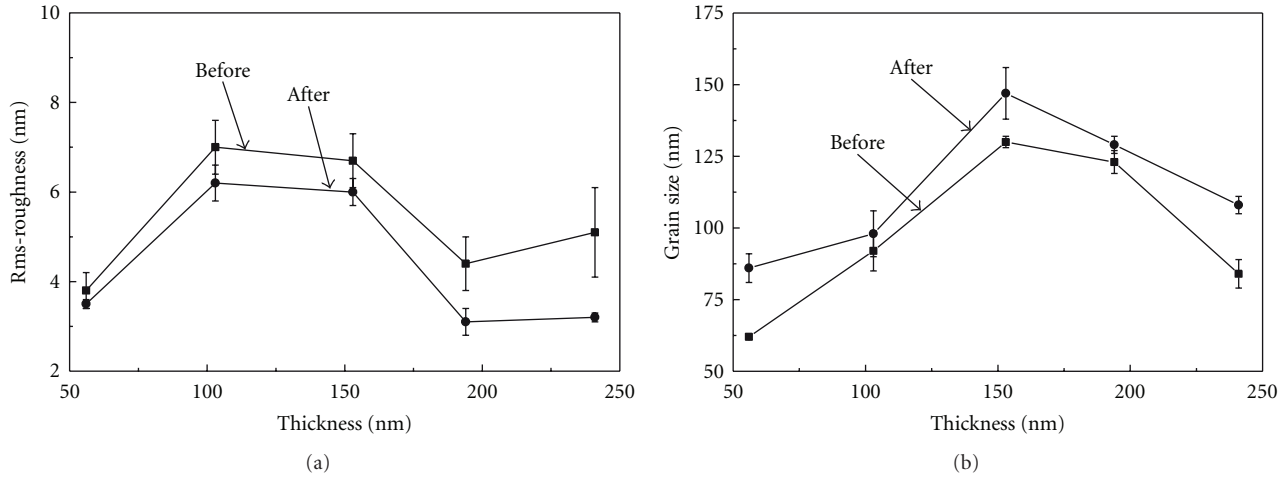

Figure 12: Changes on the: (a) rms-roughness, and (b) grain size both before and after tensile testing.

for Cu films have been reported by other authors [23] by using an optical diffraction technique. They report this elastic modulus value for Cu in a range of 0.1 to 2.0 μm film thickness. The lower elastic modulus value obtained herein for 50 nm-thick Cu film may be explained by the lack of coalescence among grains or clusters for such a small film thickness, which seems to be particularly relevant for copper. This affirmation is also supported by the high electrical resistivity reported for Cu films of 50 nm thickness [24].

After mechanical testing, the elongated surfaces of the tested alloys were examined by SEM. SEM analysis did not show microcracks on the surface of the elongated alloys, confirming that loading was kept within the elastic regime. The surface morphology was also obtained by AFM in order to examine differences with the pristine condition (prior to testing). Figure 11 shows sequential AFM images of the Al-Cu alloys deposited with different thickness, corresponding to scenarios before and after tensile testing (images do not correspond to the same zone). As-grown images obtained from different zones of each alloy showed similar rms-roughness values, suggesting a homogeneous growth condition during evaporation.

From AFM images, the rms-roughness (R_{rms}) and the mean grain size (D_{mean}) were measured for each thickness of Al-Cu alloy both before and after tensile testing. Their corresponding mean values and standard deviations are shown in Figure 12. Both R_{rms} and D_{mean} show an initial increment with increased film thickness until maximum values are reached at alloy thickness of 150 nm; after alloy thickness of 150 nm, the R_{rms} and D_{mean} values show a slight reduction. The largest values of the roughness and grain size both before and after tensile testing were found for the 150 nm thick alloy. After deformation, the initial surface roughness value decreases, meanwhile the initial grain size increases.

After annealing (alloy formation), diffusion process and diffusion time affect the final surface of alloys given the dependence of R_{rms} and D_{mean} with the film thickness and formation temperature. In our case, the 150 nm thick Al-Cu film suffered the largest surface morphology changes may be due to the combined action of the alloy thickness, diffusion temperature, and diffusion time. The diffusion process discussed here for Al-Cu film formation was found to be a different behavior than the growth process, where according to the scaling laws, the rms-roughness value and the grain size of the surface increase with increased thickness (or deposition time) until a saturation is reached.

4. Conclusions

The elastic modulus of 50–250 nm thick Al-50 at.% Cu alloys thermally evaporated onto Kapton substrates and postformed by thermal diffusion has been investigated. Al_2Cu phase was the dominant crystalline phase formed as determined by XPS. Force-strain curves of the Al-Cu alloys were obtained by subtracting the force-strain curve of the Kapton substrate from the force-strain curve of the Al-Cu/Kapton material system, and elastic modulus was obtained from the slope of the corresponding stress-strain curves. Elastic modulus of the Al-Cu alloys decreased when the film thickness increased, and their values were determined in the range from 106.1 to 77.8 GPa for 50 to 250 nm thick alloys, respectively. The elastic modulus of the studied Al-Cu alloys was found between the corresponding bulk values of the Al and Cu films. The elastic modulus measured for 50 nm thick Al was higher than its corresponding bulk value, while the elastic modulus of 50 nm thick Cu was smaller than its bulk value. The highest values of the mean grain size and rms-roughness were found for the 150 nm thick Al-Cu alloy. Overall, application of a tensile strain/stress yielded a tendency to increase the grain size and decrease the surface roughness of the alloys. The methodology used to obtain the elastic modulus does not yield alloy microfractures because of the small strains (<1%) applied during tensile testing.

Acknowledgments

The authors thank the technical assistance given by Dora Huerta, W. Cauich, O. Ceh, P. Bartolo, and Alejandro May (CICY).

References

[1] C.-T. Huang, C.-L. Shen, C.-F. Tang, and S.-H. Chang, "A wearable yarn-based piezo-resistive sensor," *Sensors and Actuators A*, vol. 141, no. 2, pp. 396–403, 2008.

[2] S. A. Wilson, R. P. J. Jourdain, Q. Zhang et al., "New materials for micro-scale sensors and actuators. An engineering review," *Materials Science and Engineering R*, vol. 56, no. 1–6, pp. 1–129, 2007.

[3] J. D. Shi, K. H. Wu, and G. Larkins, "A Method for measuring the elastic modulus of thin films," *Materials Characterization*, vol. 38, no. 4-5, pp. 301–303, 1997.

[4] F. Ebrahimi and Z. Ahmed, "The effect of substrate on the microstructure and tensile properties of electrodeposited nanocrystalline nickel," *Materials Characterization*, vol. 49, no. 5, pp. 373–379, 2003.

[5] H.-C. Hsu, S.-C. Wu, S.-K. Hsu, Y.-C. Sung, and W.-F. Ho, "Effects of heat treatments on the structure and mechanical properties of Zr-30Ti alloys," *Materials Characterization*, vol. 62, no. 2, pp. 157–163, 2011.

[6] J. H. Han, M. C. Shin, S. H. Kang, and J. W. Morris, "Effects of precipitate distribution on electromigration in Al-Cu thin-film interconnects," *Applied Physics Letters*, vol. 73, pp. 762–764, 1998.

[7] C. M. Tan and A. Roy, "Electromigration in ULSI interconnects," *Materials Science and Engineering R*, vol. 58, no. 1-2, pp. 1–75, 2007.

[8] F. Habashi, *Alloy: Preparation, Properties, Application*, Edited by Q.C. Fathi Habashi, chapter 10, Wiley-VCH, 1998.

[9] V. Zolotorevsky, N. Belov, and M. Glazoff, *Casting Aluminum Alloys*, chapter 1, Elsevier, 2007.

[10] A. I. Oliva, J. E. Corona, and V. Sosa, "AlCu alloy films prepared by the thermal diffusion technique," *Materials Characterization*, vol. 61, no. 7, pp. 696–702, 2010.

[11] S. S. Babu, M. K. Miller, J. M. Vitek, and S. A. David, "Characterization of the microstructure evolution in a nickel base superalloy during continuous cooling conditions," *Acta Materialia*, vol. 49, no. 20, pp. 4149–4160, 2001.

[12] T. B. Massalski, L. F. Vassamillet, and Y. Bienvenu, "Metastable phase relationships in zinc-rich copper and silver alloys produced by rapid freezing," *Acta Metallurgica*, vol. 21, no. 5, pp. 649–661, 1973.

[13] G. Schmitz, C. B. Ene, and C. Nowak, "Reactive diffusion in nanostructures of spherical symmetry," *Acta Materialia*, vol. 57, no. 9, pp. 2673–2683, 2009.

[14] D. L. Beke, A. I. Szabo, Z. Erdelyi, and G. Opposits, "Diffusion-induced stresses and their relaxation," *Materials Science and Engineering A*, vol. 387–389, pp. 4–10, 2004.

[15] D. Gupta, "Diffusion in several materials relevant to Cu interconnection technology," *Materials Chemistry and Physics*, vol. 41, no. 3, pp. 199–2005, 1995.

[16] S. Lee, W. L. Wang, and J. R. Chen, "Diffusion-induced stresses in a hollow cylinder: constant surface stresses," *Materials Chemistry and Physics*, vol. 64, no. 2, pp. 123–130, 2000.

[17] E. Huerta, A. I. Oliva, J. E. Corona, and J. González-Hernández, "Mechanical properties of AlCu alloys thin films prepared by thermal diffusion," in *Proceedings of the 8th International Conference onElectrical Engineering, Computing Science and Automatic Control*, pp. 1042–1047, Mérida, México, 2011.

[18] E. Huerta, J. E. Corona, A. I. Oliva, F. Avilés, and J. González-Hernández, "Universal testing machine for mechanical properties of thin materials," *Revista Mexicana de Fisica*, vol. 56, no. 4, pp. 317–322, 2010.

[19] F. Macionczyk and W. Brückner, "Tensile testing of AlCu thin films on polyimide foils," *Journal of Applied Physics*, vol. 86, no. 9, pp. 4922–4929, 1999.

[20] L. B. Hazell, "Quantitative XPS analysis of aluminium in the presence of copper," *Surface and Interface Analysis*, vol. 33, no. 10-11, pp. 791–795, 2002.

[21] J. P. Lokker, A. J. Böttger, W. G. Sloof, F. D. Tichelaar, G. C. A. M. Janssen, and S. Radelaar, "Phase transformations in Al-Cu thin films: precipitation and copper redistribution," *Acta Materialia*, vol. 49, no. 8, pp. 1339–1349, 2001.

[22] P. Enghag, *Encyclopedia of the Elements*, Wiley-VCH Verlag GmbH & Co. KGaA, Weinheim, Germany, 2004.

[23] D. Y. W. Yu and F. Spaepen, "The yield strength of thin copper films on Kapton," *Journal of Applied Physics*, vol. 95, no. 6, pp. 2991–2997, 2004.

[24] J. M. Camacho and A. I. Oliva, "Morphology and electrical resistivity of metallic nanostructures," *Microelectronics Journal*, vol. 36, no. 3–6, pp. 555–558, 2005.